

Large Area TOF-SIMS Imaging of the Antibacterial Distribution in Frozen-Hydrated Contact Lenses

Overview: Imaging by time-of-flight secondary ion mass spectrometry (TOF-SIMS) is accomplished in a vacuum environment. In many instances the analytical specimens are innately compatible with the vacuum environment which consists of pressures at $< 1.0 \times 10^{-6}$ Torr (i.e. $< 1.3 \times 10^{-4}$ Pa). Vacuum compatible samples include metals, stable oxides (some oxides will reduce in a vacuum environment), semiconductors, intermetallics, nonvolatile organics, and most bulk and thin film polymers. However, there are several classes of samples that require precise thermal control while exposed to the vacuum environment to prevent the evaporation of volatile species from the surface. Examples include high vapor pressure organics in either bulk or thin films, labile polymers, hydrated polymers, and hydrated biological specimens, to name a few. Thermal control of such samples is required because evaporation of volatile species from the surface may alter the sample morphology, disturb the surface chemical distribution, and change the 3D chemical distribution.

It is not sufficient to simply cool a hydrated sample to cryogenic temperatures, e.g. to -130 °C [1]. The reason that a particular sample should not be over-cooled is related to the vacuum environment. That is to say, every vacuum environment has a background comprised in part of water vapor. Therefore, cooling the sample below the temperature required to prevent sublimation of water from the surface will produce condensation of water from the vacuum system onto the sample surface. Since TOF-SIMS is a surface sensitive analytical technique and has a sampling depth of only 2 - 4 nm, condensed water vapor due to over-cooling will quickly impede the capability to collect useful chemical information from the sample. In such instances, the mass spectrum will be dominated by cluster ions of water, $(\text{H}_2\text{O})_n\text{H}^+$. There is generally an ideal temperature in the range of -80 °C to -110 °C wherein a balance is obtained between sublimation and condensation of water at the sample surface.

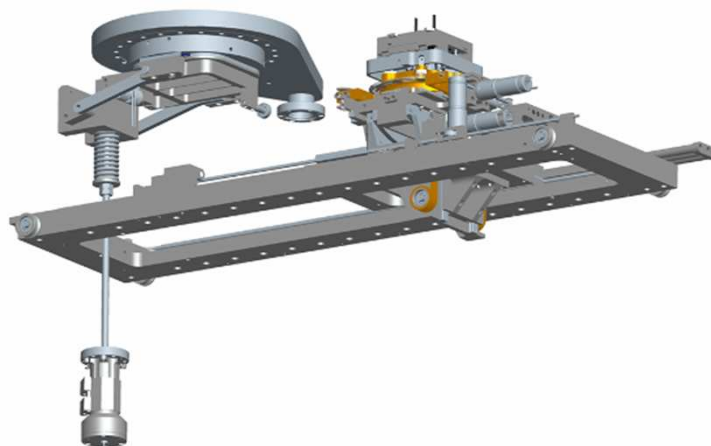


Figure 1. A schematic illustration of the 5-axis sample stage and Fast Sample Introduction chamber of the PHI nanoTOF. The specimen holder is mounted directly onto the sample stage for superior thermal control and imaging stability. The sample stage travels continuously between the Fast Sample Introduction chamber (top left), where the sample stage forms the bottom seal of the isolated Intro chamber volume, and the analysis position (at right as shown). Owing to the unique and innovative design features of the nanoTOF's patented sample stage, precise temperature control of the sample is never interrupted by sample introduction, and full 5-axis motion is available during temperature-programmed analysis.

The exercise of precise temperature control during TOF-SIMS analysis has, to date, virtually eliminated the possibility of sample motion with the exception of sample introduction. That is to say, the complete imaging capability of TOF-SIMS is restricted to a single, relatively small field-of-view. Moreover, during the few minutes of sample introduction using a conventional magnetically coupled mechanical transfer apparatus the sample temperature is neither precisely controlled nor well known. These long-accepted limitations concerning the introduction and chemical imaging of temperature-controlled specimens are eliminated by the innovative sample handling design incorporated into the PHI *nanoTOF*. A brief description of the *nanoTOF*'s modern 5-axis sample stage is provided in Figure 1.

In this Note, we demonstrate the unique capability of the PHI *nanoTOF* to obtain chemical images from large areas (e.g. several mm x several mm) of frozen-hydrated samples. The sample set consists of two hydrogel contact lenses with a 24% (w/w) water content; one lens is drug-loaded with Ciprofloxacin and one lens has no drug loading. The patented design of the *nanoTOF*'s sample stage provides full 5-axis sample motion concurrently with precise control of the sample temperature. Additionally, because the sample is mounted directly onto the sample stage, the sample temperature is controlled during the few minutes of fully automated sample introduction as well as during TOF-SIMS analysis.

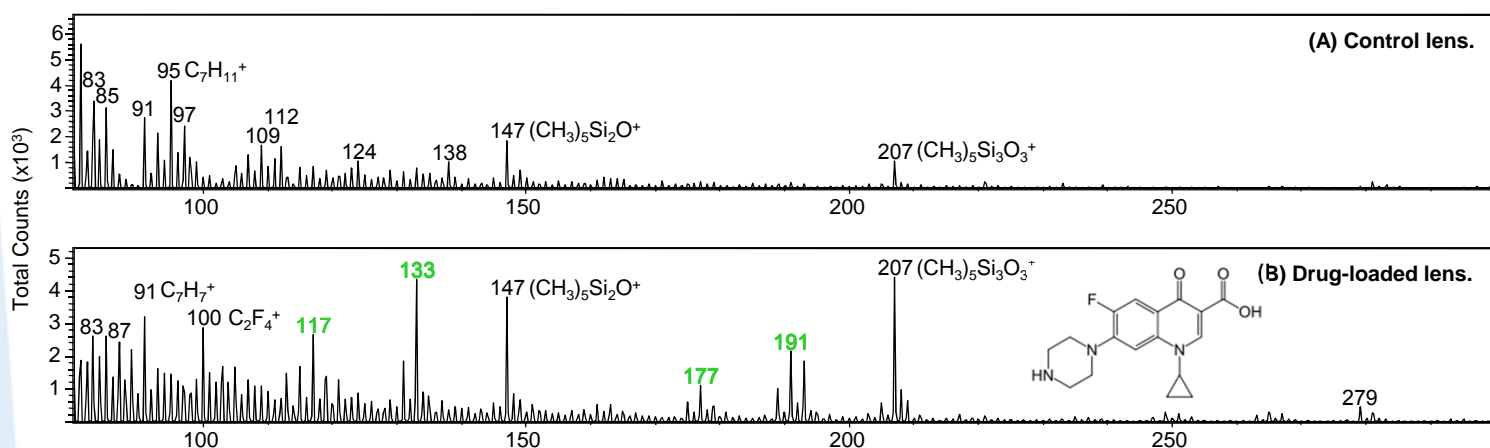


Figure 2. Positive secondary ion polarity (+SIMS) mass spectra of the control (A) and the drug-loaded (B) hydrogel lenses in the mass range of 80 – 300 m/z. The structure of the drug, Ciprofloxacin, is inset. Several molecular fragment ions of the matrix components are indicated along with their composition, and molecular fragment ions of the drug Ciprofloxacin are indicated by bold green font. Notice that peaks arising from condensed water do not dominate the mass spectra of either the control or the drug-loaded lens specimens although they are necessarily present at modest levels due to the 24% (w/w) water content of the hydrogel matrix. The differences in relative signal intensities may be related to a matrix effect caused by the presence or absence of the drug in the respective sample matrix.

Experimental: The hydrogel contact lens samples were stored in saline solution prior to analysis. Each lens sample was mounted and analyzed in turn. For mosaic (large area) imaging by TOF-SIMS, the whole, intact lens was mounted onto the cryogenic specimen holder which was then mounted onto the *nanoTOF*'s sample stage at the Intro chamber. After mounting the cryogenic specimen holder onto the sample stage, the hydrogel sample was cooled to -10 °C in the Intro chamber under a N₂ gas purge to minimize water condensation onto the sample surface. Once a sample temperature of -10 °C was achieved, the automated sample introduction was initiated and the sample was simultaneously cooled to a temperature of -80 °C. The duration of sample cooling, pumpdown and introduction was approximately 40 minutes.

A bunched 30 keV Au⁺ primary ion beam was used to acquire chemical images of the hydrogel lens specimens. TOF-SIMS image data was collected only in the positive secondary ion polarity because all the chemistries of interest were present with strong positive ion yields. A raw data stream file was collected to allow further post-acquisition evaluation (i.e. retrospective analysis) of the data. All data were collected operating the Au⁺ primary ion beam at DC current of 1.5 nA. The mosaic image is defined by the primary ion beam field-of-view (FOV), the digital raster being 256 pixels x 256 pixels, and the number of tiles in the X and Y directions.

Each mosaic image tile was collected by scanning the primary ion beam over a 400 μm field-of-view per tile, and the resulting primary ion dose density (PIDD) was $2.9 \times 10^{12} \text{ Au}^+/\text{cm}^2$ per tile; the stage is then moved in 400 μm increments between tiles. The data collection time is dependent on both the total area of the mosaic image and the data collection time per tile of the mosaic image. For the $4.4 \times 3.6 \text{ mm}^2$ area imaged of the control lens, the total acquisition time was 45 minutes; for the $2.4 \times 4.8 \text{ mm}^2$ area imaged of the drug-loaded lens, the total acquisition time was 35 minutes. Charge compensation of the insulating specimens during analysis was accomplished using PHI's patented dual-beam charge neutralization technology.

Results: The hydrogel lenses that were interrogated in this study are comprised of perfluoroether (PFE), tris(trimethylsiloxy) silylpropylmethacrylate (TRIS), and N,N-dimethylacrylamide (DMA). Copper Phthalocyanine (CuPc) is also present in the hydrogel as a tinting agent. The presence of these chemical moieties may each be identified by the respective secondary ion species of CF^+ (31 m/z), CF_3^+ (69 m/z) and C_2F_4^+ (100 m/z) for the PFE, Si^+ (28 m/z), $(\text{CH}_3)_3\text{Si}^+$ (73 m/z), $(\text{CH}_3)_5\text{Si}_2\text{O}^+$ (147 m/z) and $(\text{CH}_3)_5\text{Si}_3\text{O}_3^+$ (207 m/z) for the TRIS, $\text{C}_2\text{H}_5\text{N}^+$ (43 m/z) for the DMA, and Cu^+ (63 and 65 m/z) and C_7H_7^+ (91 m/z) for the CuPc. It should be noted that this list of secondary ion species for each matrix component is not exhaustive. The corresponding mass spectra, with notable chemical features in the range of 80 – 300 m/z being indicated for the purposes of comparing the control and the drug-loaded lenses, are given in Figure 2. For several of the more intense features the composition is also indicated.

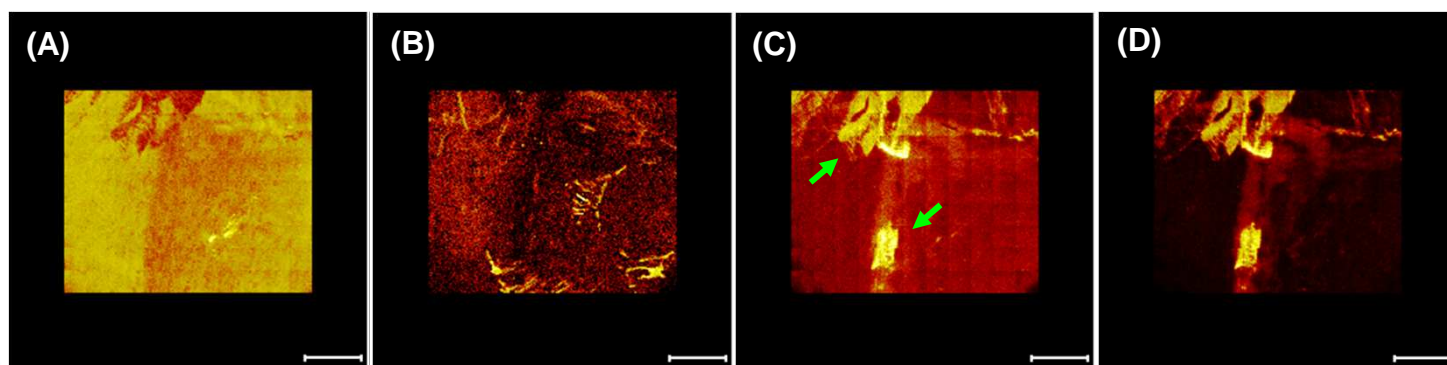


Figure 3. Mosaic (large area) TOF-SIMS images of the control hydrogel lens acquired at -80°C . The FOV is $4.4 \times 3.6 \text{ mm}^2$ (scale bar is 1 mm). (A) Mosaic image of Na^+ (23 m/z). (B) Mosaic image of CF^+ (31 m/z). (C) Mosaic image of C_3H_5^+ (41 m/z). (D) Mosaic image of $\text{C}_2\text{H}_5\text{N}^+$ (43 m/z). The green arrows in panel (C) indicate marks in the lens material that were caused during sample mounting.

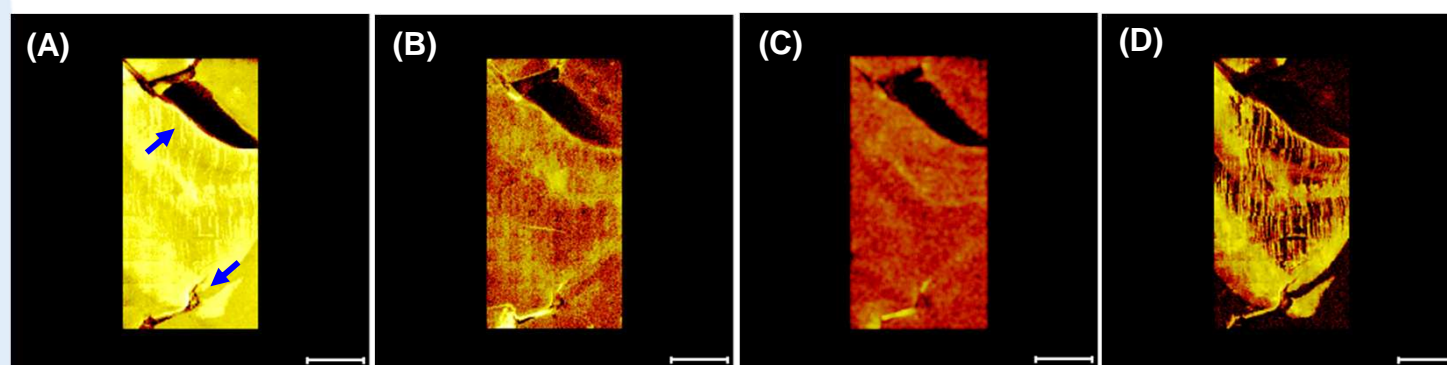


Figure 4. Mosaic (large area) TOF-SIMS images of the drug-loaded hydrogel lens acquired at -80°C . The FOV is $2.4 \times 4.8 \text{ mm}^2$ (scale bar is 1 mm). (A) Mosaic image of C_2H_3^+ (27 m/z). (B) Mosaic image of Si^+ (28 m/z). (C) Mosaic image of CF^+ (31 m/z). (D) Mosaic image of K^+ (39 m/z). The blue arrows in panel (A) indicate tears in the lens material that were caused during sample mounting.

The hydrogel lenses have, on average, a 24% (w/w) water content. It is noteworthy that the mass spectra of the lenses, pictured in Figure 2, are not overwhelmed by the presence of water cluster species (i.e. $(\text{H}_2\text{O})_n\text{H}^+$) although such secondary ions are necessarily present in each mass spectrum. The reason that $(\text{H}_2\text{O})_n\text{H}^+$ cluster ions do not dominate the mass spectra of the hydrogel lenses is because the sample temperature during introduction and analysis was maintained such that a balance was achieved between sublimation and condensation of water [1].

Ion specific mosaic images of the control hydrogel lens are shown in Figure 3. These images reveal a relatively homogeneous distribution of the hydrogel components in the contact lens matrix. There are several areas in the mosaic images where the signals of matrix components, e.g. C_3H_5^+ and $\text{C}_2\text{H}_5\text{N}^+$, are higher than surrounding areas. These areas of high signal intensity appear to be caused by damage to the lens surface that occurred during sample mounting and which has disturbed the latent surface layers to expose the underlying hydrogel matrix. That is to say, the labile fraction of siloxane that has bloomed to form a layer at the surface of the lens has been disrupted to expose the underlying chemistry. This assumption is based on the appearance of the markings in the upper portion of the mosaic images in Figures 3A, 3C and 3D; these markings have a shape that resembles the tweezers used for sample mounting. The surface distribution of the fluorocarbon moiety, i.e. CF^+ , has a different appearance which is not readily explained by damage caused during sample handling.

Ion specific mosaic images of the drug-loaded hydrogel lens are shown in Figure 4. The chemical images, as illustrated by Si^+ and CF^+ , reveal a relatively homogeneous distribution of the hydrogel components in the drug-loaded contact lens matrix; note that the C_3H_5^+ and $\text{C}_2\text{H}_5\text{N}^+$ images are not shown in Figure 4 for the drug-loaded lens. In contrast to the control lens sample, the distribution of CF^+ is quite homogeneous. There are two additional features of the mosaic images of the drug-loaded lens that must be mentioned and discussed. First, in Figure 4A, the blue arrows indicate tears in the contact lens material that were caused while mounting the sample onto the cryogenic specimen holder. These tears are observed in each ion image. Second, as observed in Figure 4D, the distribution of K^+ across the contact lens surface is quite intense and nonuniform when compared to the distribution of matrix components. An explanation for this observation is not immediately available, especially considering that both the control and the drug-loaded lenses were stored using the same saline solution. The distribution of Ca^+ (40 m/z), not shown, is nearly identical to that observed in the K^+ mosaic image.

The expected difference between the control and the drug-loaded lenses is the presence of features arising from the antibacterial agent, Ciprofloxacin. The prominent mass spectral features of the drug appear at 117 m/z , 133 m/z , 177 m/z and 191 m/z , as revealed in Figure 2B. The composition of the mass spectral features is not given, but identification is possible with an appropriate reference. Mosaic images showing the distribution of the drug as a function of surface position are given in Figure 5. Both of the molecular fragment ion images of the drug suggest a uniform distribution of the drug in the hydrogel matrix.

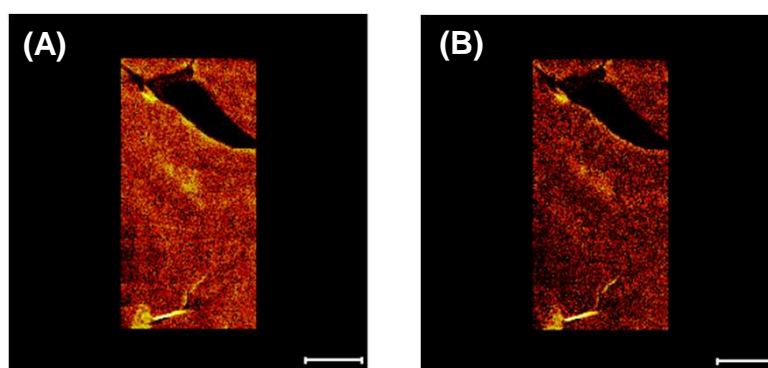


Figure 5. Mosaic (large area) TOF-SIMS images of the drug-loaded hydrogel lens acquired at $-80\text{ }^\circ\text{C}$ and showing the distribution of the drug, Ciprofloxacin, using the molecular fragment ions at (A) 133 m/z and at (B) 191 m/z . The FOV is $2.4 \times 4.8\text{ mm}^2$ (scale bar is 1 mm).

Conclusion: The unique and analytically powerful characteristics of the PHI TRIFT V *nanoTOF* were demonstrated in the context of mosaic (large area) imaging of frozen-hydrated hydrogel contact lenses. The hydrogel lenses were introduced to the vacuum system for analysis and were examined under temperature control at -80 °C to achieve equilibrium between sublimation and condensation of water. Charge neutralization was easily accomplished with PHI's patented dual-beam charge neutralization technology, and the patented sample handling allowed mosaic imaging to be performed during control of the sample temperature. In summary, large areas (several mm x several mm) of the control and the drug-loaded contact lenses were chemically imaged to reveal the distribution of matrix components. The drug was uniquely identified in the drug-loaded lens, and the distribution of the drug was observed to be reasonably uniform.

Acknowledgements & References:

We would like to thank Dr. Lyndon Jones at the University of Waterloo School of Optometry for providing the contact lens specimens.

[1] D.M. Cannon, M.L. Pacholski, N. Winograd and A.G. Ewing, *J. Am. Chem. Soc.* **122** (2000) 603.



Physical Electronics USA, 18725 Lake Drive East, Chanhassen, MN 55317
Telephone: 952-828-6200, Website: www.phi.com

ULVAC-PHI, 370 Enzo, Chigasaki City, Kanagawa 253-8522, Japan
Telephone 81-467-85-4220, Website: www.ulvac-phi.co.jp